PET/CT features of extrapulmonary tuberculosis at first clinical presentation: a cross-sectional observational ^{18}F-FDG imaging study across six countries

Jamshed Bomanji[1,14], Rajnish Sharma[2,14], Bhagwant R. Mittal[3,14], Sanjay Gambhir[4,14], Ahmad Qureshy[5,14], Shamim M.F. Begum[6,14], Diana Paez[7,14], Mike Sathekge[8,14], Mariza Vorster[8,14], Dragana Sobic Saranovic[9,14], Pawana Pusuwan[10,14], Vera Mann[1,14], Sobhan Vinjamuri[11,14], Alimuddin Zumla[12,14] and Thomas N.B. Pascual[13,14], for the International Atomic Energy Agency Extra-pulmonary TB Consortium

@ERSpublications
^{18}F-FDG PET/CT can localise EPTB disease sites not clinically detected. It may serve a useful tool for research studies defining pathogenetic mechanisms and cure, relapse and recurrence. http://bit.ly/2CKSH9a

Cite this article as: Bomanji J, Sharma R, Mittal BR, *et al*. PET/CT features of extrapulmonary tuberculosis at first clinical presentation: a cross-sectional observational ^{18}F-FDG imaging study across six countries. *Eur Respir J* 2020; 55: 1901959 [https://doi.org/10.1183/13993003.01959-2019].

ABSTRACT

Background: A large proportion of the huge global burden of extrapulmonary tuberculosis (EPTB) cases are treated empirically without accurate definition of disease sites and extent of multi-organ disease involvement. Positron emission tomography (PET) imaging using 2-deoxy-2-(fluorine-18) fluoro-D-glucose (^{18}F-FDG) in tuberculosis could be a useful imaging technique for localising disease sites and extent of disease.

Methods: We conducted a study of HIV-negative adult patients with a new clinical diagnosis of EPTB across eight centres located in six countries: India, Pakistan, Thailand, South Africa, Serbia and Bangladesh, to assess the extent of disease and common sites involved at first presentation. ^{18}F-FDG PET/computed tomography (CT) scans were performed within 2 weeks of presentation.

Findings: 358 patients with EPTB (189 females; 169 males) were recruited over 45 months, with an age range of 18–83 years (females median 30 years; males median 38 years). 350 (98%) out of 358 patients (183 female, 167 male) had positive scans. 118 (33.7%) out of 350 had a single extrapulmonary site and 232 (66.3%) out of 350 had more than one site (organ) affected. Lymph nodes, skeleton, pleura and brain were common sites. 100 (28%) out of 358 EPTB patients had ^{18}F-FDG PET/CT-positive sites in the lung. 110 patients were ^{18}F-FDG PET/CT-positive in more body sites than were noted clinically at first presentation and 160 patients had the same number of positive body sites.

Interpretation: ^{18}F-FDG PET/CT scan has potential for further elucidating the spectrum of disease, pathogenesis of EPTB and monitoring the effects of treatment on active lesions over time, and requires longitudinal cohort studies, twinned with biopsy and molecular studies.

Received: 08 Oct 2019 | Accepted after revision: 11 Nov 2019

Introduction

Background and rationale

Tuberculosis (TB) remains the leading infectious disease cause of death worldwide [1]. The annual global incidence of TB cases in 2017 was reported to be 10 million, of which an estimated 15% were extrapulmonary TB (EPTB). These figures may be an underestimate, since EPTB is a neglected clinical problem worldwide [2–5] and the diagnosis of EPTB can be overlooked easily due to nonspecific symptoms, chronic and cryptic protean clinical manifestations, low clinician awareness of the possibility of TB and lack of an accurate tool for detection of extrapulmonary disease sites [4, 5]. Up to 45% of the global burden of EPTB remains undiagnosed and untreated [1, 6]. Furthermore, definitions traditionally used for clinical presentations of TB have been generally classified by the World Health Organization (WHO) as pulmonary TB (PTB) and extrapulmonary TB (EPTB). A large proportion of patients with EPTB are started on anti-TB treatment (ATT) empirically upon clinical suspicion, utilising current WHO management guidelines without an accurate definition of specific disease site(s) and extent of multi-organ involvement.

Positron emission tomography (PET) imaging using 2-deoxy-2-(fluorine-18) fluoro-D-glucose (^{18}F-FDG) can provide functional information on sites with active inflammatory and immune cells that utilise glucose [7]. Acquiring ^{18}F-FDG PET and computed tomography (CT) data together combines anatomical and functional information in one scan [8]. Preliminary studies of TB in macaques [9] and humans [10–13] using ^{18}F-FDG PET/CT as a research tool have indicated that it could have clinical applications as a imaging technique for localising disease sites.

Objectives

We performed a cross-sectional observational study under operational conditions in six countries to assess the potential clinical usefulness of ^{18}F-FDG PET/CT in 1) localising disease site(s); 2) defining the extent of disease; and 3) identifying common sites involved at first presentation.

Methods

Study design

A multi-centre, cross-sectional observational study.

Setting and study centres

The study was conducted at eight centres approved by the International Atomic Energy Agency located in six countries: India (Delhi, Chandigarh and Lucknow), Pakistan (Lahore), Thailand (Bangkok), South Africa (Pretoria), Serbia (Belgrade) and Bangladesh (Dhaka).

Ethics/institutional review board approval

Study protocols were approved by the relevant local institutional review boards/ethics committees.

Participants and patient eligibility criteria

The selection of patients and the study referral pathway are outlined in figures 1 and 2.

Inclusion criteria

1) Age ⩾18 years; 2) negative HIV test; 3) patients with previous TB who had completed their treatment and been labelled as cured ⩾6 months previously; and 4) WHO criteria for EPTB [13, 14] met with one of

Affiliations: [1]Institute of Nuclear Medicine, UCLH NHS Foundation Trust, London, UK. [2]Division of Nuclear Medicine and PET Imaging, Specialist in Nuclear Medicine and Thyroid Diseases, Molecular Imaging and Research Center (MIRC), INMAS, Delhi, India. [3]Dept of Nuclear Medicine and PET, Post Graduate Institute of Medical Education and Research, Chandigarh, India. [4]Dept of Nuclear Medicine, SGPGIMS, Lucknow, India. [5]Institute of Nuclear Medicine and Oncology (INMOL) Hospital, Lahore, Pakistan. [6]National Institute of Nuclear Medicine and Allied Sciences (NINMAS), BSM Medical University Campus, Shahbag, Bangladesh. [7]Nuclear Medicine and Diagnostic Imaging Section, Division of Human Health, IAEA, Vienna, Austria. [8]Dept of Nuclear Medicine, Steve Biko Academic Hospital, University of Pretoria, Pretoria, South Africa. [9]Faculty of Medicine University of Belgrade, Center of Nuclear Medicine Clinical Center of Serbia, Belgrade, Serbia. [10]Division of Nuclear Medicine, Faculty of Medicine, Siriraj Hospital, Mahidol University, Bangkok, Thailand. [11]Dept of Nuclear Medicine, Royal Liverpool University Hospital, Liverpool, UK. [12]Center for Clinical Microbiology, Division of Infection and Immunity, University College London, and the National Institute of Health Research Biomedical Research Centre at UCL Hospitals, London, UK. [13]Section of Nuclear Medicine and Diagnostic Imaging, Division of Human Health, Dept of Nuclear Sciences and Applications, International Atomic Energy Agency, Vienna International Centre, Vienna, Austria. [14]All authors contributed equally.

Correspondence: Jamshed Bomanji, Institute of Nuclear Medicine, 5th Floor, UCLH NHS Foundation Trust, 235 Euston Road, London NW1 2BU, UK. E-mail: jamshed.bomanji@nhs.net

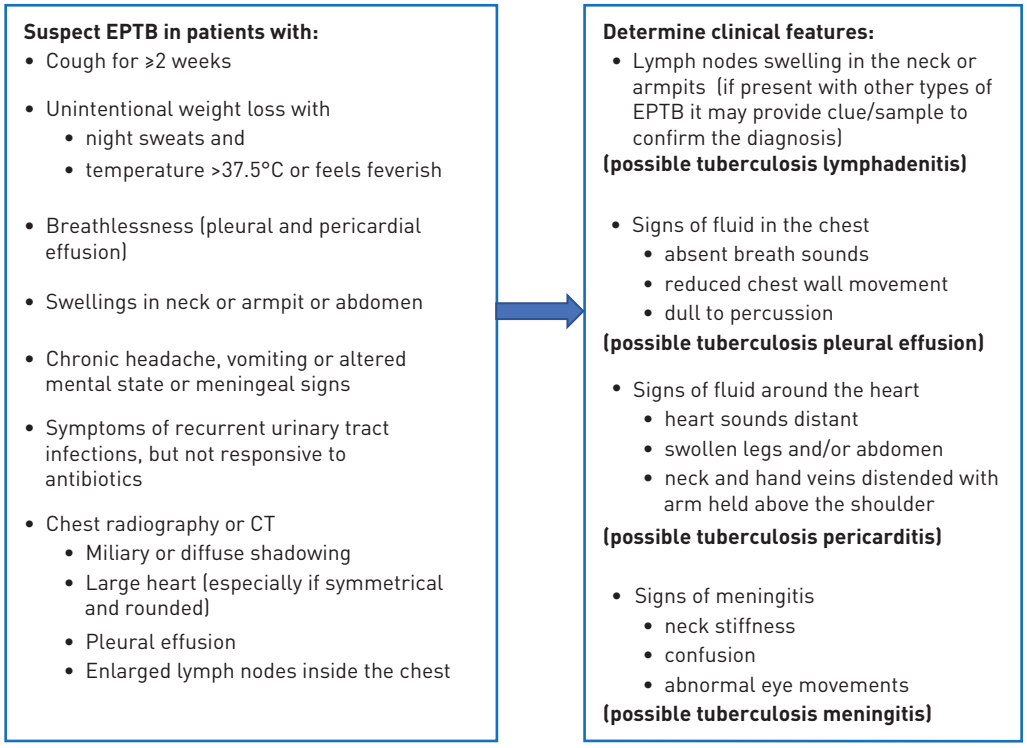

FIGURE 1 Clinical guide used to assist in the diagnosis of extrapulmonary tuberculosis (EPTB) [14]. CT: computed tomography.

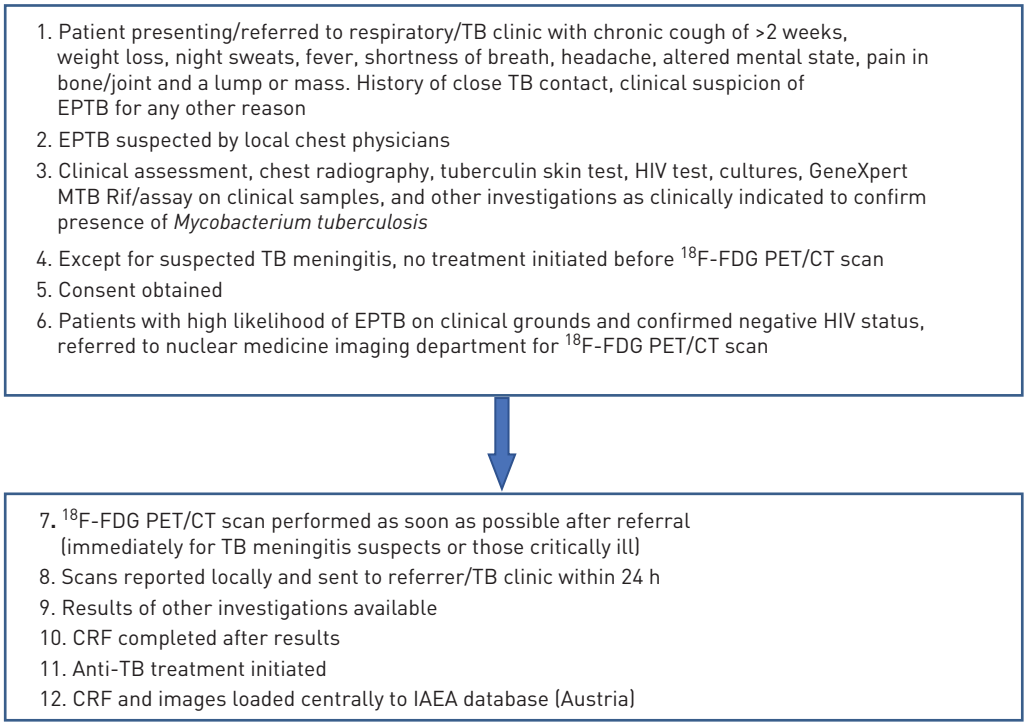

FIGURE 2 Clinical selection criteria and referral pathway algorithm. TB: tuberculosis; EPTB: extrapulmonary TB; ^{18}F-FDG: 2-deoxy-2-(fluorine-18) fluoro-D-glucose; PET: positron emission tomography; CT: computed tomography; CRF: case report form; IAEA: International Atomic Energy Agency.

the following: a positive culture for *Mycobacterium tuberculosis*, in any clinical specimen, a positive nucleic acid amplification culture GeneXpert MTB Rif/Assay (Cepheid, Sunnyvale, CA, USA) from any clinical specimen or a histopathological diagnosis of TB.

Exclusion criteria

1) Pregnant and lactating patients; 2) positive HIV test; 3) history of cancer or currently undergoing radiotherapy or chemotherapy; 4) receipt of anti-TB treatment at the time of presentation; 5) known multidrug-resistant TB (MDR-TB); 6) blood glucose levels $\geqslant$11 mmol·L^{-1} or $\geqslant$200 mg·dL^{-1}; 7) use of systemic investigational drugs; and 8) any social condition that the investigator believed would warrant exclusion.

ATT

Newly diagnosed EPTB patients were started on WHO-recommended ATT regimens [15] of 6 months' duration, except in patients with bone and central nervous system involvement, in whom they were continued for 9–12 months based on clinical response.

^{18}F-FDG PET/CT scans and procedure

^{18}F-FDG PET/CT scans were performed according to international guidelines [8]. PET/CT scanners used were the General Electric Discovery STE (BGO Detector; General Electric, Milwaukee, WI, USA) with 16-slice CT scanner at the Pakistan, India, Bangladesh and Thailand sites and Siemens mCTBiograph (CPS, Knoxville, TN, USA), 64-slice PET/CT at the Serbia and South Africa sites. The radiation dose for the ^{18}F-FDG PET/CT scan is ~12 mSv; this level of radiation dose is considered safe.

Interpretation of ^{18}F-FDG PET/CT scans

Scans were reported as positive or negative. A positive scan was defined as abnormally increased ^{18}F-FDG uptake in a lesion (with CT correlate) which is greater than the surrounding background and not explained by normal physiological organ uptake. The increase in metabolic activity was quantified by measuring the standardised uptake values (SUV_{max}), which are a relative measure of FDG metabolism: $SUV = \frac{r}{(a'/w)}$ where r=radioactivity concentration (kBq·mL^{-1}), a′=is the decay-corrected amount of radiolabelled FDG (kBq) and w=weight of patient (g). A SUV_{max} of $\geqslant$2.5 was considered as ^{18}F-FDG PET-positive. Scan reports were made available within 24 h to the referring study clinician.

Statistical analysis

Descriptive statistics were used to summarise patients' characteristics. For continuous variables, median and interquartile ranges (IQR) are given, and for categorical variables, proportions falling into different categories were calculated. Statistical analysis was performed using Stata version 15 (SE 15 data version; StataCorp, College Station, TX, USA).

Results

Study population

Figure 3 depicts a patient enrolment chart. A total of 358 patients with EPTB (189 females; 169 males) were recruited across the eight centres in six countries from April 2014 to December 2017. Age range was 18–83 years (females 18–83 years, median 30 years, IQR 23–48 years; males 18–81 years, median 38 years, IQR 27–54 years). The geographical origin of study patients is shown in figure 4. Of the 189 female patients, 17 were from Africa, 158 from Asia (India, Pakistan, Bangladesh and Thailand) and 14 from Serbia. Of the 169 male patients, eight were from Africa, 152 from Asia and nine from Serbia. Clinical features at enrolment are shown in figure 5 and table 1. There was no difference in anatomical distribution patterns across geographical sites. No adverse effect was observed due to injection of ^{18}F-FDG, during scanning and on follow-up a week after scanning.

Baseline anatomical distribution of ^{18}F-FDG PET/CT-positive EPTB sites

Table 2 depicts the anatomical location of PET/CT-positive sites and SUV_{max} values in all 358 patients. Of the 358 patients, 350 (98%; 183 female, 167 male) had a positive scan, of whom 118 (33.7%) had a single extrapulmonary site and 232 (66.3%) more than one site (organ). Lymph nodes, skeleton, pleura and brain were common sites.

Clinical versus *PET/CT findings*

110 patients were ^{18}F-FDG PET/CT-positive at more body sites than had been noted clinically at first presentation. In 160 patients the suspected clinical site was confirmed as diagnosed clinically with no additional sites involved, while 80 showed fewer sites than had been suspected clinically. Figure 6 shows an example of a positive ^{18}F-FDG PET/CT scan due to pericardial TB which was missed clinically.

First baseline scan at enrolment (n=358)

(within 2 weeks of diagnosis)

- Females (n=189) (age 18–83 years median 30 years)
- Males (n=169) (age 18–81 years median 38 years)

Active lesions

- 1 site 118 patients
- 2 sites 96 patients
- 3 sites 53 patients
- 4 sites 41 patients
- >4 sites 42 patients

FIGURE 3 Patient demographics and number of active lesions on positron emission tomography/computed tomography scan.

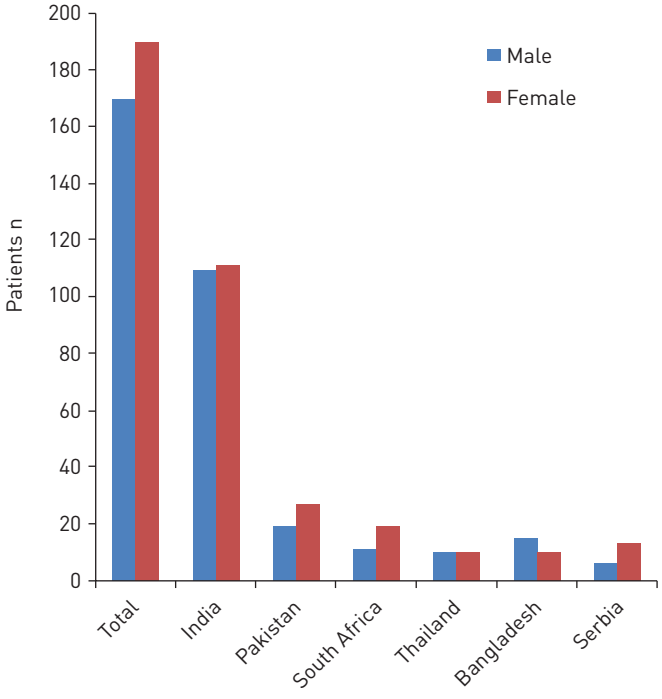

FIGURE 4 Study population: geographical distribution and sex.

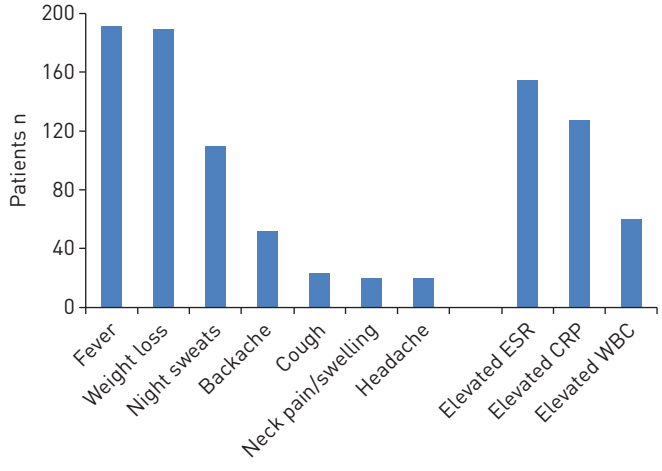

FIGURE 5 Clinical features at first enrolment. ESR: erythrocyte sedimentation rate; CRP: C-reactive protein; WBC: white blood cells.

TABLE 1 Clinical and laboratory characteristics of 358 patients at enrolment

Participants	358
Sex	
Male	169 (47)
Female	189 (53)
Age years	33 (18–83)
History of previous TB (stopped TB treatment 6 months previously)	28 (7.8)
Investigations	
Positive sputum culture for *M. tuberculosis*	28 (7.8)
EPTB specimen *M. tuberculosis* culture positive (*e.g.* ascites, CSF, pleural, synovial fluid)	75 (20.9)
M. tuberculosis biopsy positive	180 (50.2)
Elevated white cell count	60 (16.8)
Elevated ESR	155 (43.3)
Elevated CRP	126 (35.2)
Positive ^{18}F-FDG PET/CT scan	350/358 (97.8)

Data are presented as n, n (%), median (range) or n/N (%). TB: tuberculosis; *M. tuberculosis*: *Mycobacterium tuberculosis*; CSF: cerebrospinal fluid; ESR: erythrocyte sedimentation rate; CRP: C-reactive protein; ^{18}F-FDG: 2-deoxy-2-(fluorine-18) fluoro-D-glucose; PET: positron emission tomography; CT: computed tomography.

EPTB with concomitant PTB

100 (28%) out of 358 EPTB patients had ^{18}F-FDG PET/CT positive sites in the lung. PTB was not suspected at enrolment in 28 of these. Figure 7 shows an example of missed pulmonary disease in a patient initially diagnosed as having lymph node EPTB.

TABLE 2 Baseline first positron emission tomography (PET)/computed tomography (CT) scan: positive 2-deoxy-2-(fluorine-18) fluoro-D-glucose (^{18}F-FDG) PET/CT extrapulmonary disease sites in 358 patients

	PET/CT-positive patients n (%)	SUV_{max}		
		Range	Mean	Median
Brain	34 (9.5)	4.0–19.0	10.0	10.0
Cardiac	2 (0.6)	3.2–13.8	8.5	8.5
Pleura	34 (9.5)	2.6–17.7	7.1	6.7
Muscles[#]	10 (2.8)	2.8–15.9	7.4	6.7
Liver	7 (2.0)	3.8–23.3	12.4	13.1
Spleen	11 (3.1)	2.7–20.1	5.2	3.5
Gastrointestinal tract	8 (2.2)	3.4–17.4	4.8	9.3
Urogenital tract	7 (2.0)	2.6–16.9	9.7	10.0
Bone	151 (42.2)	2.5–32.8	9.5	8.1
Lymph nodes	225 (62.8)	2.8–32.3	10.7	9.9
Cervical	108 (30.2)	2.6–22.3	8.2	7.2
Supraclavicular	69 (19.3)	3.1–24.4	8.4	6.9
Axillary	51 (14.2)	2.5–20.0	7.1	5.8
Mediastinal	152 (42.4)	2.5–21.2	6.9	5.9
Hilar	70 (19.6)	2.7–23.0	6.3	5.3
Retrocrural	9 (2.5)	2.7–15.7	6.4	5.3
Retroperitoneal/mesenteric	55 (15.4)	3.0–16.1	7.0	6.4
Pelvic	28 (7.8)	2.5–21.5	6.9	6.4
Inguino-femoral	18 (5.0)	2.5–11.5	5.7	5.0
Other sites[¶]	21 (5.9)	2.5–32.0	7.5	5.7

Some patients had more than one organ involved. SUV_{max}: maximum standardised uptake value; SUV_{max} is a relative measure of FDG metabolism: $SUV = \frac{r}{(a'/w)}$; r: radioactivity concentration (kBq·mL^{-1}); a′: decay-corrected amount of radiolabelled FDG (kBq); w: weight of patients (g). [#]: iliopsoas n=4, pectoral muscle n=1, posterior intercostal n=1, gluteal n=2, thigh n=1, obturator internus n=1; [¶]: paravertebral mass/collection n=12 (SUV_{max} 2.5–9.8), adrenals n=3 (SUV_{max} 3.9–6.5), joint effusions n=3 (SUV_{max} 12.9–32), endometrium/ovary n=2 (SUV_{max} 4.1–7.1), focal bone marrow lesion n=1 (SUV_{max} 5.2).

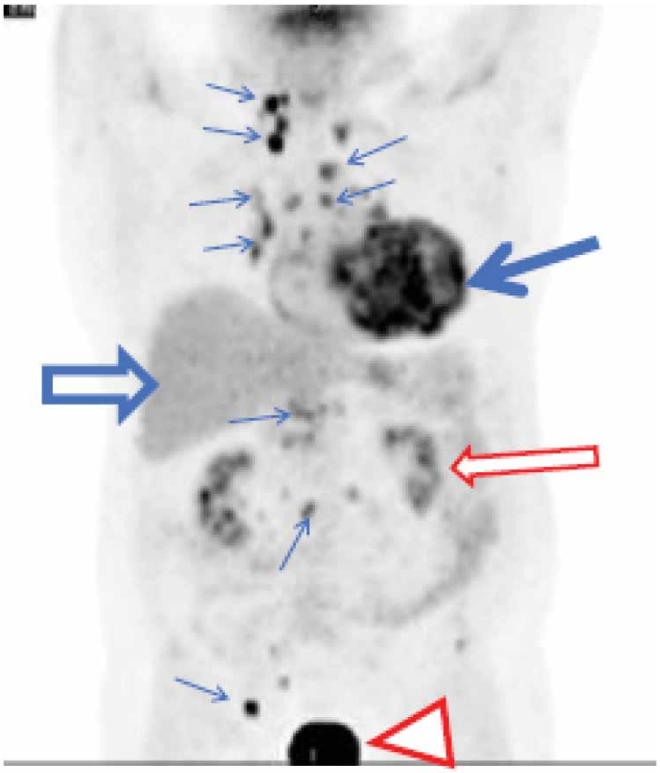

FIGURE 6 2-deoxy-2-(fluorine-18) fluoro-D-glucose (^{18}F-FDG) positron emission tomography (PET)/computed tomography (CT) scan showing disease involvement of the pericardium missed at presentation. Pericardial activity is demonstrated (large blue closed arrow), as are lymph node stations above and below the diaphragm (small blue arrows). Normal metabolic activity is noted in the liver (open arrow, blue) and excreted activity is observed in the kidneys (open arrow, red) and urinary bladder (open arrowhead, red).

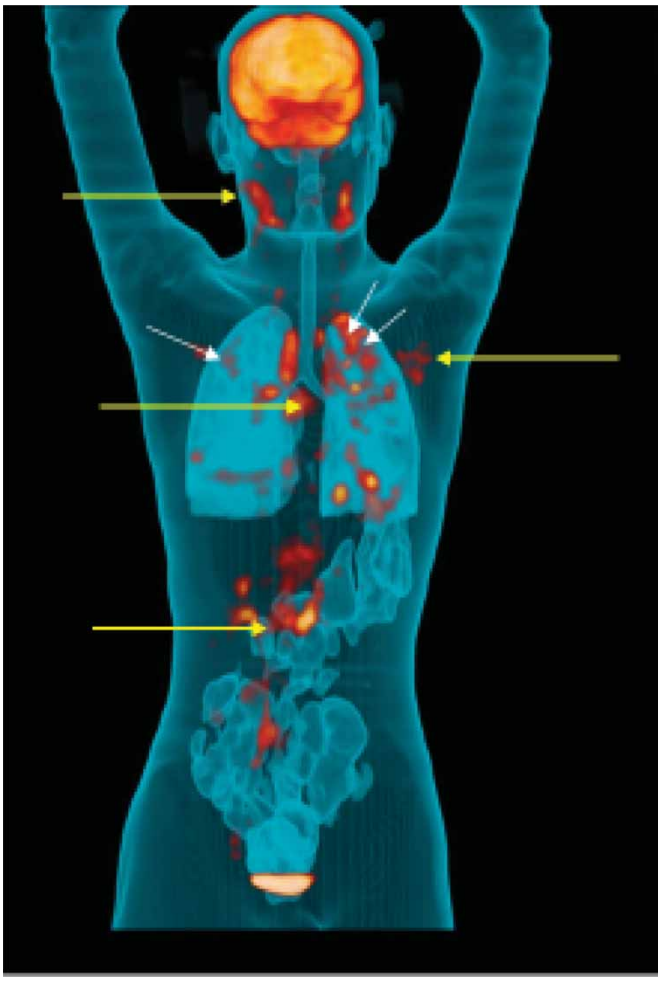

FIGURE 7 2-deoxy-2-(fluorine-18) fluoro-D-glucose (^{18}F-FDG) positron emission tomography (PET)/computed tomography (CT) scan showing nodal extrapulmonary tuberculosis and unexpected pulmonary tuberculosis (PTB). Whole-body projection is shown. The yellow arrows indicate, from top to bottom, ^{18}F-FDG uptake in the bilateral cervical nodes, axillary nodes, subcarinal nodes and retroperitoneal nodes. Small white arrows indicate PTB.

^{18}F-FDG PET/CT negative scans

Eight out of 358 patients showed low-grade uptake below the positive cut-off (SUV_{max} <2.5) and were classified as scan-negative. In two patients, there was diffuse leptomeningeal disease (SUV_{max} 1.8 and 2.1), and one of the two had a ring-enhancing lesion in the left temporal region. Four had lesions in the spine and hips (SUV_{max} 1.7–2.1) and two had abdominal TB, with low-grade metabolism noted in ascitic fluid, thickened omentum and mediastinal lymph nodes (SUV_{max} <2.5).

Discussion

This study is the largest cross-sectional observational cohort PET/CT study from six countries of HIV-negative adult patients with a diagnosis of EPTB. ^{18}F-FDG PET/CT scans were performed at first clinical presentation. The data obtained further inform the current dialogue and debate on the clinical usefulness of PET/CT as an imaging tool for defining extent of disease and aiding management. There are several notable findings from our study:

First, ^{18}F-FDG PET/CT scan detected EPTB sites in 98% of EPTB cases enrolled.

Second, more extrapulmonary active sites were detected compared with the number suspected clinically at first diagnosis of EPTB. This study reaffirms the spatial and temporal heterogeneity of TB lesions previously demonstrated in smaller single-centre studies.

Third, pulmonary involvement was more frequently found than was considered at first clinical presentation. Our study detected more pulmonary sites than were suspected at first admission, thereby raising again the vexed issue of definitions traditionally used for clinical presentations of TB. These have been generally classified by the WHO as PTB and EPTB [14]; the former being assumed to be more common. A patient with both PTB and EPTB is classified by the WHO as a case of mixed PTB and not EPTB, while intrathoracic TB lymphadenitis or pleural effusion constitutes a case of EPTB. EPTB specifically refers to TB involving organs other than the lungs, such as pleura, lymph nodes, gastrointestinal tract, urogenital tract, bones and joints, liver, spleen, meninges and brain (examples from our study are shown in figures 6–9). Global estimates of the incidence, prevalence and treatment outcomes of EPTB are inaccurate, and the WHO [1] acknowledges that there is a large undiagnosed burden of EPTB, and that current estimated data are unreliable, due to current definitions of EPTB and PTB.

Our study focused on HIV-negative patients in the first instance to exclude confounding factors of comorbidities and co-infections. However, in difficult-to-treat clinical situations such as EPTB in HIV patients, detection of extrapulmonary lesions may be particularly useful, since these could be due to various infectious or non-infectious complications of HIV/AIDS. In these individuals obtaining tissue or fluid for analysis from cryptic sites may not always be possible. Detection of active inflammatory sites by ^{18}F-FDG PET/CT offers opportunities for identifying disease sites and obtaining tissue biopsies for microbiological, molecular investigations and for understanding EPTB pathogenesis. In animal TB model studies an increase in ^{18}F-FDG activity, reflected as SUV_{max} values, was found to be proportional to the number of *M. tuberculosis* bacilli in caseating granulomas [16]. However, PET/CT findings only reflect inflammatory activity and do not identify the underlying specific microbial or other causes.

Our study was observational and there are several limitations to the acquisition and interpretation of our data. PET/CT technology has been in use for more than a decade for scanning cancer patients, albeit only in large tertiary centres. By design, ^{18}F-FDG PET/CT scans detect glucose metabolism and therefore are not specific for the detection of TB lesions and cannot differentiate between TB infection, co-infection and tumours [17]. Detection of brain tuberculomas and meningeal involvement is difficult, since, as our data show, the normal brain grey matter shows relatively high uptake due to cerebral cortical metabolic activity. Furthermore, if the lesions are small ($\leqslant$1 cm), they are very likely to be missed due to partial volume effects. Larger and metabolically more active lesions are easily detected. Interpretation of PET/CT of kidneys and urinary bladder is limited, since these organs contribute to physiological ^{18}F-FDG tracer excretion and the intensity of uptake is sufficiently high to mask small lesions. ^{18}F-FDG PET/CT therefore has low sensitivity in detecting small EPTB lesions in the kidney and urinary bladder, and conventional imaging should be used to identify lesions when urological TB is suspected. An important area where the role of ^{18}F-FDG PET/CT requires evaluation is childhood TB. Diagnosis and management of EPTB in this age group remains challenging, and further work is needed to address this. Currently, most cases of childhood TB are missed, while in diagnosed cases empirical treatment is instituted. Obtaining non-invasive clinical samples in children is difficult and microbiological diagnosis of childhood EPTB requires tissue biopsy; even then microbiological confirmation is achieved in only a small proportion of treated cases. ^{18}F-FDG PET/CT is now being assessed for the detection of TB lesions and assessment of disease activity in children [18].

Accurate microbiological diagnosis of EPTB is hindered by the difficulty in obtaining clinical samples from relatively inaccessible sites. Sentinel autopsy studies from Africa have shown a significant

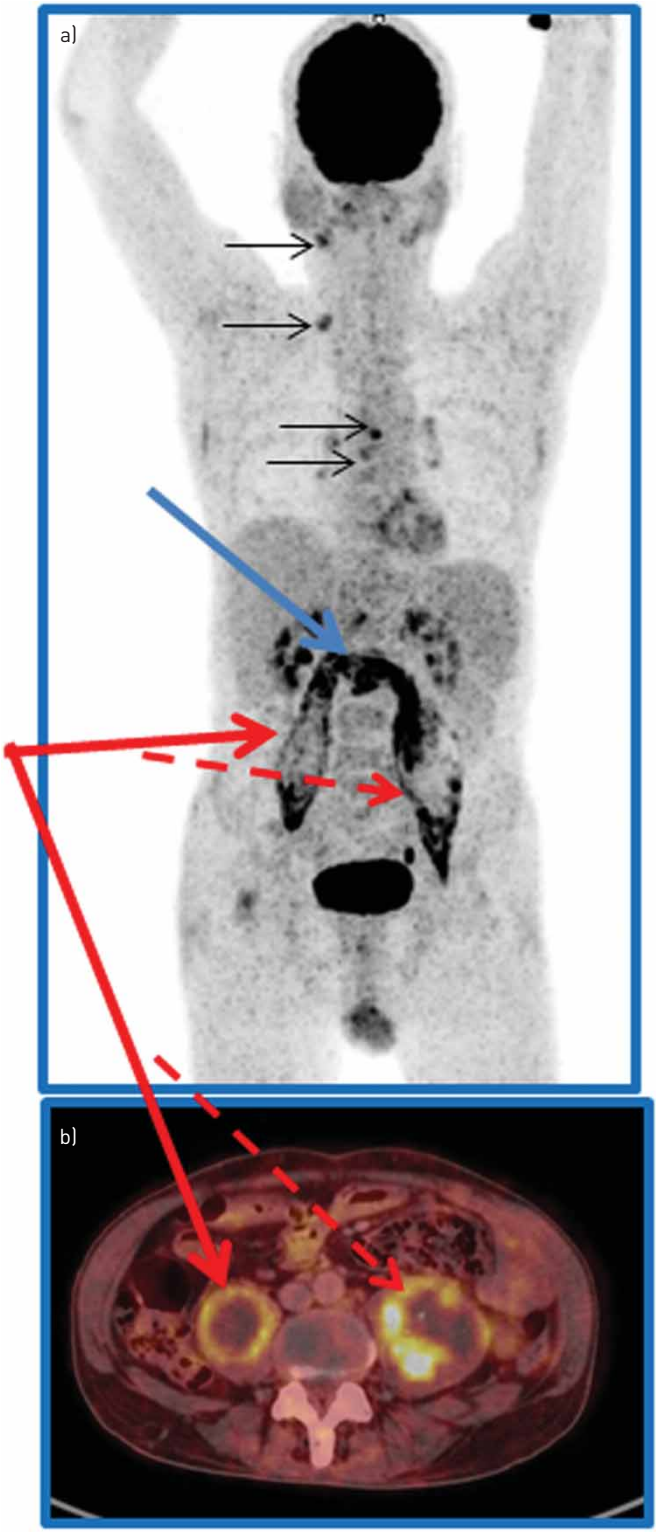

FIGURE 8 2-deoxy-2-(fluorine-18) fluoro-D-glucose (^{18}F-FDG) positron emission tomography (PET)/computed tomography (CT) scan showing nodal, bone and muscle involvement from extrapulmonary tuberculosis. a) Whole-body projections of ^{18}F-FDG PET/CT scan shown with corresponding b) transaxial fused slices (PET and CT) at areas of interest. ^{18}F-FDG PET revealing intense ^{18}F-FDG avidity in the L1-L2 vertebrae (blue arrow), with bilateral psoas abscess (red arrows) and few mediastinal and cervical lymph nodes (small black arrows).

undiagnosed burden of EPTB and PTB in adults and children antemortem [19–22]. Clinicopathological discrepancies have been identified in identifying the underlying cause(s) cause of death in adults with many missed cases of TB [21]. A recent autopsy study from Mozambique [22] of 223 deaths (57 maternal deaths, 112 adults and 54 children) showed that *M. tuberculosis* DNA can be identified using molecular methods despite absence of TB lesions on histology. In a study of 150 individuals suspected of having cancer, biopsy of pulmonary nodules localised by PET/CT identified 10 cases of active TB, with nine having SUV_{max} above the threshold of 2.5 [23]. There is a need for accurate imaging to localise sites of

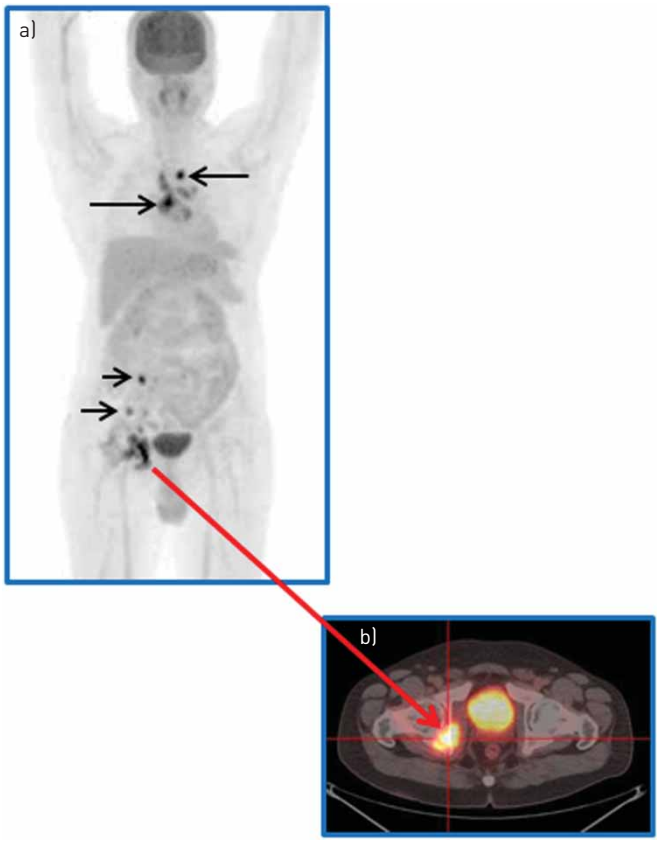

FIGURE 9 2-deoxy-2-(fluorine-18) fluoro-D-glucose (^{18}F-FDG) positron emission tomography (PET)/computed tomography (CT) scan showing nodal and acetabular extrapulmonary tuberculosis. Whole-body projections from ^{18}F-FDG PET scan: a) large black arrows indicate ^{18}F-FDG uptake in mediastinal nodes; small black arrows indicate uptake in right iliac nodes; b) red arrow indicates involvement of right posterior acetabular bone, shown in axial section.

disease activity which can be targeted to obtain clinical samples for microbiological and pathological analyses.

Currently there are several ongoing studies on the application of PET/CT and other modalities for insight into pathogenesis [24]. These include studies on spectrum of latent TB infection, subclinical disease and paucibacillary disease. Studies of EPTB patients with sequential serial scans during the course of treatment may provide further information on the usefulness of PET/CT in predicting or monitoring response to therapy, defining cure and detecting relapse [24].

The current challenge for TB-specific PET/CT is the development of new *M. tuberculosis*-specific tracers targeting high-density surface epitopes, gene targets or metabolic pathways. A recent study developed a multidrug treatment model in rabbits with experimentally induced TB meningitis and performed serial dynamic ^{11}C-rifampin PET over 6 weeks, demonstrating that rifampicin penetration into infected brain lesions is limited and spatially heterogeneous and decreases rapidly as early as 2 weeks into treatment [25]. These data demonstrate the proof of concept of ^{18}F-FDG PET/CT as a clinically translatable imaging tool for measurement of intralesional antimicrobial distribution in infected tissues that might be useful in establishing individualised treatment regimens.

Translation of ^{18}F-FDG PET/CT into a diagnostic tool for resource-poor countries will remain a vexed and challenging issue. The technology is relatively expensive compared with some conventional imaging modalities. Innovation will be needed to reduce the cost and complexity if it is to be used as a tool in patients with high-risk or confirmed EPTB. It is likely that PET/CT will be useful in Western countries with a low TB incidence and in tertiary-care facilities in high TB-endemic areas and research facilities. The limited availability of PET/CT and limited facilities for production of isotope and high cost (~USD 800–1000 per scan) make the use of PET/CT in developing countries unlikely in the near future. Thus, PET/CT will remain a research tool for TB and will not have any significant impact on the day-to-day management of the majority of patients in high TB-endemic countries.

Conclusions

^{18}F-FDG PET/CT shows promise as a useful imaging technique for detecting the extent of EPTB disease and detects more extrapulmonary and pulmonary active sites compared with the number suspected

clinically at first diagnosis of EPTB. The potential of ^{18}F-FDG PET/CT in further elucidating the spectrum of disease, the pathogenesis of EPTB and monitoring the effects of treatment on active lesions over time, including in HIV-infected, paediatric and MDR-TB patients requires longitudinal cohort studies of those with microbiologically confirmed and clinically suspected cases, twinned with biopsy and molecular studies over longer periods.

Acknowledgements: We thank Olga Morozova (International Atomic Energy Agency (IAEA) Vienna, Austria), who provided organisational backup and collated the case report forms.

Author contributions: J. Bomanji, T.N.B Pascual and A. Zumla developed the concept and initiated discussions which led to the formation of the consortium. All authors developed and helped finalise the study protocols. R. Sharma, B.R. Mittal, S. Gambhir, A. Qureshy, S.M.F. Begum, M. Sathekge, M. Vorster, D. Sobic Saranovic and P. Pusuwan led the study sites. S. Vinjamuri conducted quality assessment of imaging data. V. Mann performed the data analyses. J. Bomanji led the imaging studies, and with A. Zumla, D. Paez and T.N.B Pascual developed the first and subsequent drafts of the manuscript. All authors contributed to data interpretation and writing of the manuscript.

Conflict of interest: J. Bomanji was the PI and received non-financial support from IAEA, Vienna, during the conduct of the study. R. Sharma reports grants and non-financial support for research from IAEA, Vienna, during the conduct of the study. B.R. Mittal reports grants and non-financial support for research from IAEA, Vienna, during the conduct of the study. S. Gambhir reports grants and non-financial support from IAEA, Vienna, during the conduct of the study. A. Qureshy reports grants and non-financial support for research from IAEA, Vienna, during the conduct of the study. S.M.F. Begum reports grants and non-financial support for research from IAEA, Vienna, during the conduct of the study. D. Paez has nothing to disclose. M. Sathekge reports grants from International Atomic Energy association (IAEA), during the conduct of the study. M. Vorster reports grants from International Atomic Energy Association (IAEA), during the conduct of the study. D. Sobic Saranovic reports grants and non-financial support from IAEA, Vienna, during the conduct of the study. P. Pusuwan reports grants and non-financial support for research from IAEA, Vienna, during the conduct of the study. V. Mann reports payment for statistical software purchase from UCLH, during the conduct of the study. S. Vinjamuri has nothing to disclose. A. Zumla has nothing to disclose. T.N.B. Pascual has nothing to disclose.

Support statement: The International Atomic Energy Agency (IAEA) assisted in selection of recruitment centres with optimal ^{18}F-FDG PET/CT imaging facilities and provided support for ^{18}F-FDG PET/CT scans, consortium meetings and centralised facilities for data storage. A. Zumla and J. Bomanji acknowledge support from the NIHR Biomedical Centre at UCL Hospitals Foundation NHS Trust. A. Zumla is a member of the Pan-African network for Rapid research, Response and Preparedness for Infectious Diseases Epidemics (PANDORA-ID-NET consortium (www.pandora-id.net/)) and acknowledges support from the PANDORA-ID-NET, EDCTP CANTAM2, TESA2 and EACCR2 grants from the European and Developing Countries Clinical Trials Partnership (EDCTP2) programme. A. Zumla is in receipt of a National Institutes of Health Research (NIHR) senior investigator award. Funding information for this article has been deposited with the Crossref Funder Registry.

References

1 World Health Organization. Global Tuberculosis Report 2018. www.who.int/tb/publications/global_report/en/ Date last accessed: October 24, 2018.
2 Sharma SK, Mohan A. Extrapulmonary tuberculosis. *Indian J Med Res* 2004; 120: 316–353.
3 Sreeramareddy CT, Panduru KV, Verma SC, *et al.* Comparison of pulmonary and extrapulmonary tuberculosis in Nepal – a hospital-based retrospective study. *BMC Infect Dis* 2008; 8: 8.
4 Ilgazli A, Boyaci H, Basyigit I, *et al.* Extrapulmonary tuberculosis: clinical and epidemiologic spectrum of 636 cases. *Arch Med Res* 2004; 35: 435–441.
5 Solovic I, Jonsson J, Korzeniewska-Koseła M, *et al.* Challenges in diagnosing extrapulmonary tuberculosis in the European Union, 2011. *Euro Surveill* 2013; 18: 20432.
6 Kulchavenya E. Extrapulmonary tuberculosis: are statistical reports accurate? *Ther Adv Infect Dis* 2014; 2: 61–70.
7 Zhuang H, Alavi A. 18-Fluorodeoxyglucose positron emission tomographic imaging in the detection and monitoring of infection and inflammation. *Semin Nucl Med* 2002; 32: 47–59.
8 Boellaard R, Delgado-Bolton R, Oyen WJ, *et al.* FDG PET/CT: EANM procedure guidelines for tumour imaging: version 2.0. *Eur J Nucl Med Mol Imaging* 2015; 42: 328–354.
9 Coleman MT, Maiello P, Tomko J, *et al.* Early changes by ^{18}fluorodeoxyglucose positron emission tomography coregistered with computed tomography predict outcome after *Mycobacterium tuberculosis* infection in cynomolgus macaques. *Infect Immun* 2014; 82: 2400–2404.
10 Martinez V, Castilla-Lievre MA, Guillet-Caruba C, *et al.* ^{18}F-FDG PET/CT in tuberculosis: an early non-invasive marker of therapeutic response. *Int J Tuberc Lung Dis* 2012; 16: 1180–1185.
11 Martin C, Castaigne C, Vierasu I, *et al.* Prospective serial FDG PET/CT during treatment of extrapulmonary tuberculosis in HIV-infected patients: an exploratory study. *Clin Nucl Med* 2018; 43: 635–640.
12 Dureja S, Sen I, Acharya S. Potential role of F18 FDG PET-CT as an imaging biomarker for the noninvasive evaluation in uncomplicated skeletal tuberculosis: a prospective clinical observational study. *Eur Spine J* 2014; 23: 2449–2454.
13 Stelzmueller I, Huber H, Wunn R, *et al.* 18F-FDG PET/CT in the initial assessment and for follow-up in patients with tuberculosis. *Clin Nucl Med* 2016; 41: e187–e194.
14 World Health Organization. Improving the Diagnosis and Treatment of Smear-Negative Pulmonary and Extrapulmonary Tuberculosis among Adults and Adolescents. 2016. www.who.int/tb/publications/2006/tbhiv_recommendations.pdf Date last accessed: October 4, 2018.
15 Gilpin C, Korobitsyn A, Migliori GB, *et al.* The World Health Organization standards for tuberculosis care and management. *Eur Respir J* 2018; 51: 1800098.

16 Lin PL, Ford CB, Coleman MT, *et al.* Sterilization of granulomas is common in both active and latent tuberculosis despite extensive within-host variability in bacterial killing. *Nat Med* 2014; 20: 75–79.
17 Niyonkuru A, Bakari KH, Lan X. ^{18}F-fluoro-2-deoxy-D-glucose PET/computed tomography evaluation of lung cancer in populations with high prevalence of tuberculosis and other granulomatous disease. *PET Clin* 2018; 13: 19–31.
18 Pelletier-Galarneau M, Martineau P, Zuckier LS, *et al.* ^{18}F-FDG-PET/CT imaging of thoracic and extrathoracic tuberculosis in children. *Semin Nucl Med* 2017; 47: 304–318.
19 Bates M, Shibemba A, Mudenda V, *et al.* Burden of respiratory tract infections at *post mortem* in Zambian children. *BMC Med* 2016; 14: 99.
20 Bates M, Mudenda V, Shibemba A, *et al.* Burden of tuberculosis at *post mortem* in inpatients at a tertiary referral centre in sub-Saharan Africa: a prospective descriptive autopsy study. *Lancet Infect Dis* 2015; 15: 544–551.
21 Ordi J, Castillo P, Garcia-Basteiro AL, *et al.* Clinico-pathological discrepancies in the diagnosis of causes of death in adults in Mozambique: a retrospective observational study. *PLoS One* 2019; 14: e0220657.
22 Garcia-Basteiro AL, Hurtado JC, Castillo P, *et al.* Unmasking the hidden tuberculosis mortality burden in a large *post mortem* study in Maputo Central Hospital, Mozambique. *Eur Respir J* 2019; 54: 1900312.
23 Heysell SK, Thomas TA, Sifri CD, *et al.* 18-Fluorodeoxyglucose positron emission tomography for tuberculosis diagnosis and management: a case series. *BMC Pulm Med* 2013; 13: 14.
24 Malherbe ST, Kleynhans L, Walzl G. The potential of imaging tools as correlates of infection and disease for new TB vaccine development. *Semin Immunol* 2018; 39: 73–80.
25 Tucker EW, Guglieri-Lopez B, Ordonez AA, *et al.* Noninvasive ^{11}C-rifampin positron emission tomography reveals drug biodistribution in tuberculous meningitis. *Sci Transl Med* 2018; 10: eaau0965.